

## Numerical simulation of the Hall effect in magnetized accretion disks with the Pluto code

Mohammad Nakhaei<sup>1,3</sup>, Ghasem Safaei<sup>1</sup> and Shahram Abbassi<sup>2,3</sup>

<sup>1</sup> School of Physics, Damghan University, P.O. Box 36715-364, Damghan, Iran

<sup>2</sup> Department of Physics, School of Sciences, Ferdowsi University of Mashhad, Mashhad, 91775-1436, Iran

<sup>3</sup> School of Astronomy, Institute for Research in Fundamental Sciences, P.O. Box 19395-5531, Tehran, Iran; [abbassi@ipm.ir](mailto:abbassi@ipm.ir)

Received 2013 April 4; accepted 2013 August 21

**Abstract** We investigate the Hall effect in a standard magnetized accretion disk which is accompanied by dissipation due to viscosity and magnetic resistivity. By considering an initial magnetic field, using the PLUTO code, we perform a numerical magnetohydrodynamic simulation in order to study the effect of Hall diffusion on the physical structure of the disk. Current density and temperature of the disk are significantly modified by Hall diffusion, but the global structure of the disk is not substantially affected. The changes in the current densities and temperature of the disk lead to a modification in the disk luminosity and radiation.

**Key words:** Hall effect — accretion disks

### 1 INTRODUCTION

The accretion process is one of the most important parts of star formation theory. Accretion disks are the birthplaces of stars and planets. The mechanism by which angular momentum is lost by the material in accretion disks is a classic problem in astrophysics. A major difficulty arises when we have a magnetic field, as the formation and evolution of the disk are greatly affected by such fields. Magnetic tension appears to be one of the main sources of torque required to transport angular momentum from the material in the disk to the environment and allow it to spiral towards the central object. In magnetohydrodynamic (MHD) simulations, it has been shown that a weak field is able to remove all of the angular momentum from the accretion flow (e.g. Price & Bate 2007; Mellon & Li 2008).

In a reasonable model of astrophysical disks, the turbulence required should be sufficiently strong to enhance the efficiency of angular momentum transport. At present, there are no generally accepted models that show how the flow in the disks is disrupted and turbulence is generated. Turbulence may be generated due to various magnetohydrodynamical instabilities which will be dominant in differentially rotating and non-uniform gaseous disks, but there are some uncertainties regarding the exact origin of turbulence and the possible roles of the magnetic field, so the problem is still controversial. Magnetorotational instability (MRI) is responsible for generating turbulence in the disk which is related to the magnetic field and the rotation of the disk (Balbus & Hawley 1991). We know that MRI can only arise if the field is not too strong, because this would suppress the instability (Urpin 1996; Kitchatinov & Rudiger 1997). Simulations of the magnetorotational instability

in disks (Hawley et al. 1995; Matsumoto & Tajima 1995; Brandenburg et al. 1995; Torkelsson et al. 1996; Arlt & Rüdiger 2001) have shown that the turbulence generated from MRI is responsible for an enhancement in the transport of angular momentum.

In a weakly ionized gas, non-ideal MHDs should be taken into account. In such a gas, the charged particles have a drift velocity with respect to neutral particles. The Lorentz force only acts on the charges and would be transmitted to the neutral particles (dusty particles) through the drag forces caused by collisions between the neutral and charged particles (e.g. Königl et al. 2010). The relative drifts of charged particles with respect to the neutral particles delineate three kinds of magnetic diffusivity: ambipolar, Hall and Ohmic. Ohmic and ambipolar diffusion dominate in regions of relatively high and low density, respectively, while Hall diffusion dominates in the intermediate regimes between ambipolar and Ohmic diffusion. We expect that Hall diffusion dominates in many regions that have molecular clouds (Wardle 2004), and in protoplanetary disks (Sano & Stone 2002a,b). The importance and type of diffusion in disks are uncertain because it is too difficult to obtain detailed observations from protoplanetary disks, particularly measurements of magnetic fields. Several investigations have been done in order to make reasonable models of the non-ideal MHD effects in protoplanetary accretion disks, in particular the Hall diffusion effect (Braiding & Wardle 2012a,b; Wardle 1999; Balbus & Terquem 2001; Liverts et al. 2007; Shadmehri 2012).

When the field is moderately strong, the Hall component represents the main contribution to the electric resistivity tensor and will produce an electric field perpendicular to both the magnetic field and the electric current. This component is non-dissipative but it can change the geometry of the magnetic field. Since performing numerical simulations of the Hall effect is difficult, the role of Hall diffusion in protoplanetary disks is neither fully understood nor explored.

In this paper, the role of Hall diffusion in the structure of protoplanetary disks and the evolution of a magnetic field are simulated using 2.5D numerical MHD simulation with the PLUTO code (Mignone et al. 2007) based on a mean field approximation (Murphy et al. 2010). We have constructed a resistive viscous accretion disk threaded by a weak magnetic field. We have adopted an initial magnetic field distribution in which the disk magnetization  $\mu = B^2 z / P$  decreases radially from the central object. As our study is based on a standard disk model, due to its thickness, the disk can be divided into small thin disks and in those ranges the magnetic field lines are almost perpendicular into the plane of the disk.

We expect that the structure of the disk, the components of current density and their properties are affected by the magnetic field configuration and Hall diffusion. In this paper we demonstrate a set of time-dependent numerical MHD simulations to analyze in detail the effect of Hall diffusion on the dynamics of accretion flow and on the components of current density. The physical structure of accretion disks and their observational properties involve various factors such as fluid viscosity, central star mass, rotation speed of materials, etc. The standard accretion disk (SAD) model shows a good agreement between obtained data and observations (Shakura & Sunyaev 1973; Frank et al. 2002), so in this study the SAD model has been adopted. Turbulence is assumed to arise from the development of magnetic instabilities that are triggered in the disk whenever a magnetic field is present (Balbus & Hawley 1991). In a special case, and not far from reality, we benefit from the azimuthal symmetry of the disk and simulate the radius and elevation in a cylindrical coordinate system. Considering heating and cooling, the accretion disk is defined by the 3D models of  $\alpha$  Keplerian accretion disks originally developed in Kluzniak & Kita (2000) and further discussed by Regev & Gitelman (2002) and Umurhan et al. (2006).

When the disk is divided into smaller meshes, the Hall effect and the generated transverse current are calculated separately for each and an interpolating function that approximates the current can be obtained inside the disk and its atmosphere. Shakoura & Sunyaev standard accretion disks dissipate the energy used in the model because a standard disk effectively radiates, and for that reason they are thin; therefore we consider  $h = \epsilon r$  and  $\epsilon = c_s / V_K$  in which  $V_K$  is the Keplerian velocity at radius  $r$  and  $c_s$  is isothermal sound speed. An  $\alpha$ -prescription is adopted for the viscosity of an accretion disk,

which has been used in hydrostatic models and its evolution is controlled by a stress tensor. With respect to viscosity, because of the slowing angular momentum of the fluid layers, we must anticipate fluid collapse toward the central core and velocity emerging in the direction perpendicular to the disk plane at the center of the disk. For magnetization of the disk, we assume the initial magnetic field and atmosphere of the disk to be functions of magnetic flux  $B = \nabla\psi \times \frac{e\phi}{r}$ .

## 2 NUMERICAL METHODS

In order to perform a numerical simulation, we use PLUTO (Mignone et al. 2007). A set of axially symmetric full viscous-resistive MHD equations in protoplanetary disks was adopted to perform 2.5D numerical simulations. In this manuscript we use the framework presented by Murphy et al. (2010), so the main equations are as follows.

The continuity equation

$$\frac{\partial \rho}{\partial t} + \nabla \cdot (\rho \mathbf{v}) = 0, \quad (1)$$

the conservation of momentum equation

$$\frac{\partial \mathbf{v}}{\partial t} + \mathbf{v} \cdot \nabla \mathbf{v} + \frac{1}{\rho} \mathbf{B} \times (\nabla \times \mathbf{B}) + \frac{1}{\rho} \nabla P = -\nabla \Phi_G, \quad (2)$$

and the conservation of energy equation

$$\frac{\partial E}{\partial t} + \nabla \cdot \left[ (E + P_t) \mathbf{v} + (\mathbf{v} \cdot \mathbf{B}) \mathbf{B} + \eta_m \mathbf{J} \times \mathbf{B} - \mathbf{v} \cdot \bar{\bar{\mathbf{T}}} \right] = S. \quad (3)$$

By adding Hall diffusivity, the induction equation becomes

$$\frac{\partial \mathbf{B}}{\partial t} + \nabla \times (-\mathbf{v} \times \mathbf{B}) = -\nabla \times \left( \eta_m \mathbf{J} + \eta_{\text{Hall}} \mathbf{J} \times \hat{\mathbf{B}} \right), \quad (4)$$

where  $\rho$  is the mass density,  $\mathbf{v}$  stands for the velocity vector and  $P_t = P + \frac{1}{2}B^2$  shows total pressure, in which  $P$  and  $\mathbf{B}$  represent pressure and magnetic field, respectively.  $\mathbf{J} = \nabla \times \mathbf{B}$  is current density,  $\eta_m$  defines the magnetic diffusivity,  $\Phi_G = -\frac{GM}{\sqrt{r^2+z^2}}$  represents the gravitational potential of the central mass and  $S = -\rho \mathbf{v} \cdot \nabla \Phi_G + L_c$  represents a source function where  $L_c$  is a cooling term. Hall diffusion is represented by  $\eta_{\text{Hall}}$ , which was adopted as follows

$$\eta_{\text{Hall}} = \frac{B}{en_e}, \quad (5)$$

where  $e$  is electron charge and  $n_e$  is the number density of charge carriers (electrons). This coefficient corresponds to the properties of conductive materials and its value depends on the type, number and characteristics of charge carriers in the flow. The value of this coefficient represents the transverse Hall resistance; a greater number of charge carriers makes the fluid be more conductive and so in this case the Hall effect does not have a significant role. To understand the effect of Hall diffusion on the structure of the accretion disk we adopt three values for  $\frac{1}{en_e}$  that are equal to 0, 5.0 and 10.0. Bigger values of this parameter correspond to a lower number density for the charge carrier and consequently more influence from the Hall effect. The viscous stress tensor is defined by the following relation

$$\bar{\bar{\mathbf{T}}} = \eta_\nu \left[ (\nabla \mathbf{v}) + (\nabla \mathbf{v})^T - \frac{2}{3} (\nabla \cdot \mathbf{v}) \mathbf{I} \right], \quad (6)$$

where  $\eta_\nu$  is the dynamical viscosity and kinematic viscosity is defined as  $\nu_\nu = \frac{\eta_\nu}{\rho}$ . Following Murphy et al. (2010), in order to define the initial magnetic field, we use the magnetic flux function  $\psi$  instead of the magnetic field,  $\mathbf{B}$ , where  $\mathbf{B} = \frac{\nabla\psi \times \mathbf{e}_\phi}{r}$ . We have assumed magnetic flux to be

$$\psi(r, z) = 4B_0 r_0^2 \left(\frac{r}{r_0}\right)^{\frac{1}{4}} \frac{m^{\frac{7}{4}}}{\left(m^2 + \left(\frac{z}{r}\right)^2\right)^{\frac{7}{8}}}, \quad (7)$$

so that  $B_0 = \sqrt{\mu_0 \mu(r_0) P_{d_0}}$  and  $P_{d_0}$  is the thermal pressure of the disk. The parameter  $m$  is the initial bending of the magnetic field lines which is set to 0.935 in the simulation, as was adopted by Murphy et al. (2010).  $\mu$  is the disk magnetization at  $z = 0$  which changes as  $2 \times 10^{-3} \frac{r_0}{r}$ .

In order to perform the simulation we need initial conditions, which were taken from the perturbative solution of the steady-state MHD equations. For the initial structure of the disk, density and pressure are assumed as the following, as adopted by Murphy et al. (2010)

$$\rho_d = \rho_{d_0} \left\{ \frac{2}{5\epsilon^2} \left[ \frac{r_0}{R} - \left(1 - \frac{5\epsilon^2}{2}\right) \frac{r_0}{r} \right] \right\}^{\frac{3}{2}}, \quad (8)$$

$$p_d = p_{d_0} \left( \frac{\rho_d}{\rho_{d_0}} \right)^{\frac{5}{3}}, \quad (9)$$

in which  $p_{d_0} = \epsilon^2 \rho_{d_0} V_{K_0}^2$  where  $\epsilon = \frac{c_s}{V_K}$  is the aspect ratio of the disk and is given by the ratio between the isothermal sound speed and the Keplerian speed calculated in the disk mid-plane.

The three components of the speed are employed as

$$v_{rd} = -\alpha_v \epsilon^2 \left[ 10 - \frac{32}{3} \Lambda \alpha_v^2 - \Lambda \left( 5 - \frac{z^2}{\epsilon^2 r^2} \right) \right] \sqrt{\frac{GM}{r}}, \quad (10)$$

$$v_{\phi d} = \left[ \sqrt{1 - \frac{5\epsilon^2}{2}} - \frac{2}{15} \epsilon^2 \alpha_v^2 \Lambda \left( 1 - \frac{6z^2}{5\epsilon^2 r^2} \right) \right] \sqrt{\frac{GM}{r}}, \quad (11)$$

$$v_{zd} = v_{rd} \frac{z}{r}, \quad (12)$$

where  $\Lambda = \frac{11}{5} / \left(1 + \frac{64}{25} \alpha_v^2\right)$  and for the atmosphere above the disk we have set the values of all velocity components to zero. Furthermore, we set the pressure and density of the atmosphere as

$$\rho_a = \rho_{a_0} \left(\frac{r_0}{R}\right)^{\frac{1}{\gamma-1}}, \quad (13)$$

$$p_a = \rho_{a_0} \frac{\gamma-1}{\gamma} \frac{GM}{r_0} \left(\frac{r_0}{R}\right)^{\frac{1}{\gamma-1}}. \quad (14)$$

In order to have a reasonable density contrast in all the simulations we used  $\rho_{a_0}/\rho_{d_0} = 10^{-4}$ . We will apply the  $\alpha$  prescription for the disk's viscosity. So, following Zanni & Ferreira (2009) we use the viscous expression as

$$\nu_v = \frac{2}{3} \alpha_v \left[ c_s^2(r, z=0) + \frac{2}{5} \left( \frac{GM}{R} - \frac{GM}{r} \right) \right] \sqrt{\frac{r^3}{GM}}. \quad (15)$$

In order to have faster simulations and follow the evolution of the disk under the Hall effect we adopt a large value for the viscosity parameter,  $\alpha_v = 0.9$ . The mesh grid which we have used for this simulation consists of 256 homogeneous cells in the radial direction ( $128 r_0$ ) and 720 cells in the  $z$  direction ( $375 r_0$ ), where  $r_0$  is the inner radius of the disk.

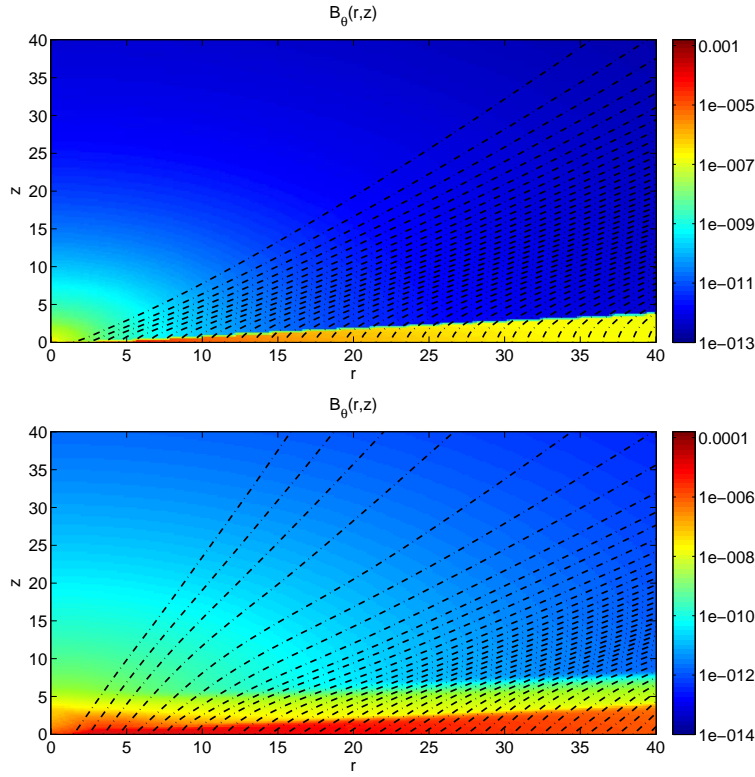


**Fig. 1** Log of Intensity of an angular magnetic field overplotted with magnetic field lines for  $\eta_{\text{Hall}} = 0.0$ . Upper panel is at time  $t = 0\tau_{K_0}$  and lower panel is at time  $t = 250\tau_{K_0}$ .

### 3 RESULTS

In this section, we present the simulations of the a thin magnetized disk under effects of viscosity, a magnetic field and Hall resistivity. All of the presented results are 2.5D numerical MHD simulations based on a mean field approximation using the PLUTO code. To perform the simulations we need to normalize all the quantities. All the parameters have been normalized with  $r_0$ , the inner radius of the disk and its corresponding quantities. Density, pressure and magnetic field strength are normalized by  $\rho_{d_0}$ ,  $\rho_{d_0} V_{K_0}^2$  and  $\sqrt{\mu_0 \mu} (r_0) P_{d_0}$ , respectively. As we stated in the last section, the velocities have been normalized by the Keplerian velocity,  $\sqrt{\frac{GM}{r_0}}$ , so for the time steps we will use Keplerian orbital period  $\tau_{K_0} = 2\pi r_0 / V_{K_0}$ .

After running the program, which takes a relatively long time, we have set a new output file in a prescribed format for the PLUTO code to see the influence of the Hall transverse resistance. We run the program with 250 Keplerian rounds in the internal radius of the disk and plot output values for the coefficients. As is clear from the induction equation, the Hall transverse resistance mainly affects the magnetic field, so, as a consequence, current density will be affected by changes in the magnetic field, through the MHD equations. We perform the simulations for  $\eta_{\text{Hall}} = 0, 1.0$  and  $10.0$ . In Figure 1 we have demonstrated the initial conditions of the system (upper panel) and its structure in  $t = 250\tau_{K_0}$ .

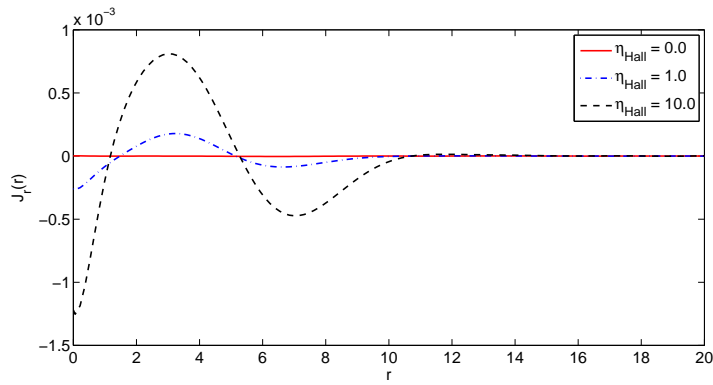


**Fig. 2** The radial current density in the middle of the disk for  $\eta_{\text{Hall}} = 0.0$ ,  $\eta_{\text{Hall}} = 1.0$  and  $\eta_{\text{Hall}} = 10.0$  at time  $t = 25.0 \tau_{K_0}$ .

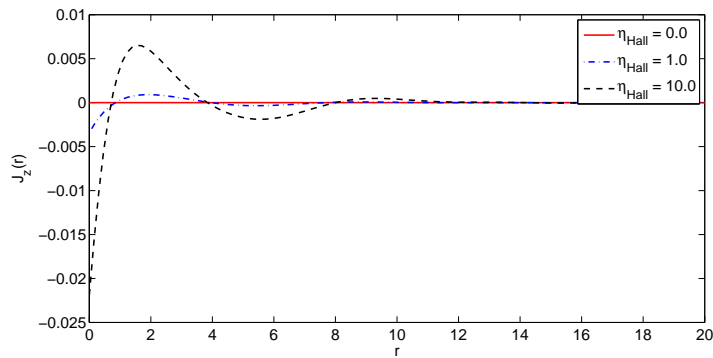
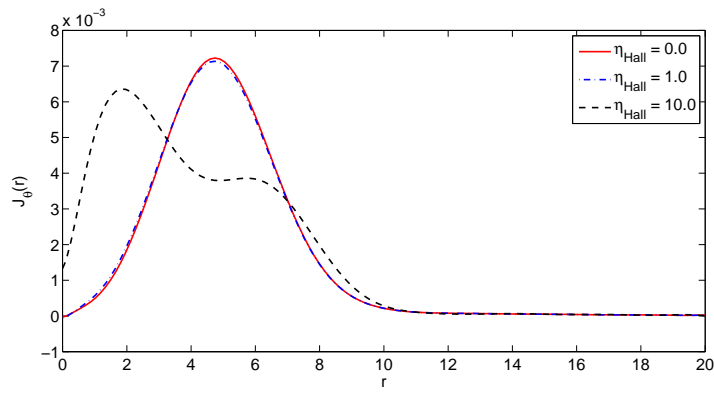


**Fig. 3** The  $\hat{z}$  component of the current density in the middle of the disk for  $\eta_{\text{Hall}} = 0.0$ ,  $\eta_{\text{Hall}} = 1.0$  and  $\eta_{\text{Hall}} = 10.0$  at time  $t = 250 \tau_{K_0}$ .

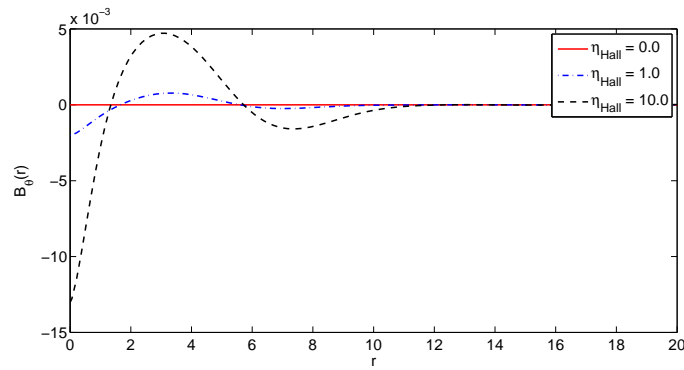
As shown in Figures 2 and 3 for the case  $\eta_{\text{Hall}} = 0.0$ , when the Hall effect does not have a significant role, current density in directions of  $\hat{r}$  and  $\hat{z}$  is zero after  $70 \tau$ . In these cases, the number of charge carriers is large and conductivity of the fluid is quite high, so Hall diffusion does not have an important role. However, by adding  $\eta_{\text{Hall}}$ , which means adding the Hall diffusion, a transverse current will penetrate with its amplitude increasing with an increasing Hall coefficient. This induced current will be dampened far from the inner boundary of the disk, because the role of the magnetic field is dominant in the inner part of the disk.

Figure 4 shows the toroidal component of current density at different radii. Adding  $\eta_{\text{Hall}}$  causes the toroidal current to shift to the inner part of the disk. This decrement in current density emerges in other directions and produces current density in the  $\hat{z}$  and  $\hat{r}$  directions. However, Figure 4 shows a small change when  $\eta_{\text{Hall}} = 1.0$ , but for  $\eta_{\text{Hall}} = 10$  the change is considerable.

The behavior of the magnetic field for all considered values of  $\eta_{\text{Hall}}$  is investigated. Figure 5 shows the vertical profiles of the toroidal component of the magnetic field for different radii when  $\eta_{\text{Hall}} = 0, 1.0$  and  $10$ . The symmetry of the original poloidal magnetic configuration implies that the toroidal field generated due to the Hall effect is anti-symmetric with respect to the equatorial plane.



**Fig. 4** The component of the toroidal current density in the middle of the disk for  $\eta_{\text{Hall}} = 0.0$ ,  $\eta_{\text{Hall}} = 1.0$ , and  $\eta_{\text{Hall}} = 10.0$  at time  $t = 250 \tau_{K_0}$ .



**Fig. 5** The toroidal component of the magnetic field in the middle of the disk for  $\eta_{\text{Hall}} = 0.0$ ,  $\eta_{\text{Hall}} = 1.0$  and  $\eta_{\text{Hall}} = 10.0$  at time  $t = 250 \tau_{K_0}$ .

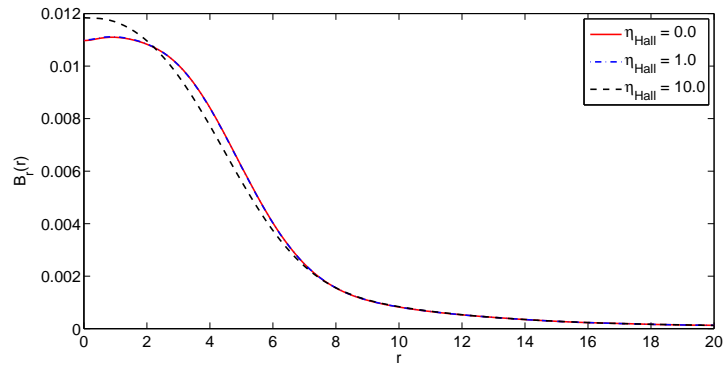


**Fig. 6** The  $r$ -component of the magnetic field in the middle of the disk for  $\eta_{\text{Hall}} = 0.0$ ,  $\eta_{\text{Hall}} = 1.0$  and  $\eta_{\text{Hall}} = 10.0$  at time  $t = 250 \tau_{K_0}$ .

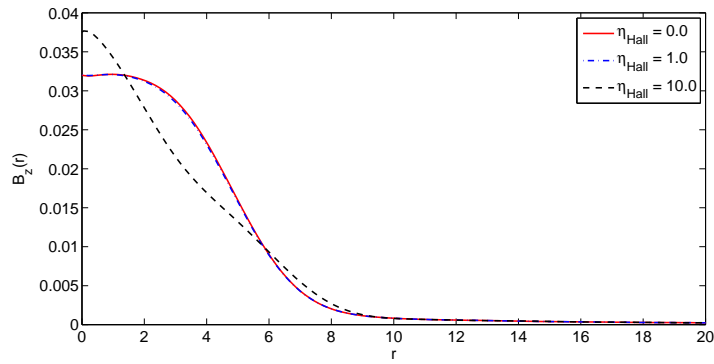


**Fig. 7** The  $z$ -component of the magnetic field in the middle of the disk for  $\eta_{\text{Hall}} = 0.0$ ,  $\eta_{\text{Hall}} = 1.0$  and  $\eta_{\text{Hall}} = 10.0$  at time  $t = 250 \tau_{K_0}$ .

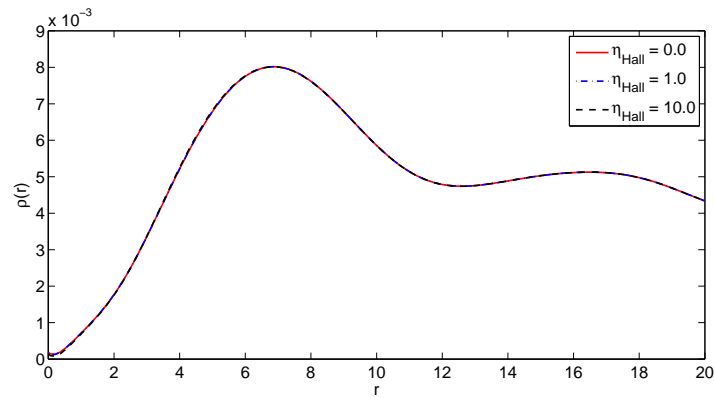


**Fig. 8** The mass density in the middle of the disk for  $\eta_{\text{Hall}} = 0.0$ ,  $\eta_{\text{Hall}} = 1.0$  and  $\eta_{\text{Hall}} = 10.0$  at time  $t = 250 \tau_{K_0}$ .

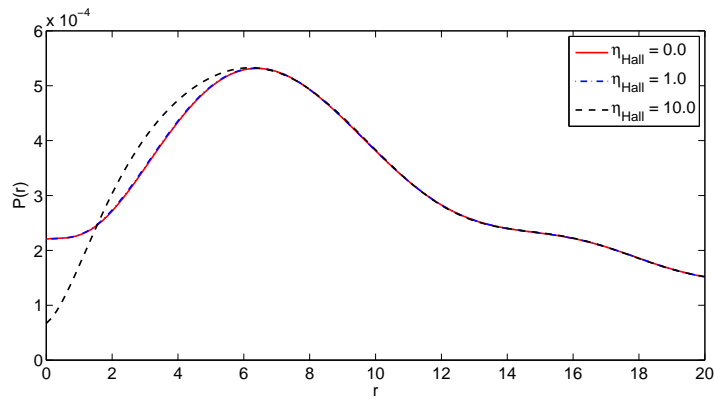


**Fig. 9** The pressure in the middle of the disk for  $\eta_{\text{Hall}} = 0.0$ ,  $\eta_{\text{Hall}} = 1.0$  and  $\eta_{\text{Hall}} = 10.0$  at time  $t = 250 \tau_{K_0}$ .

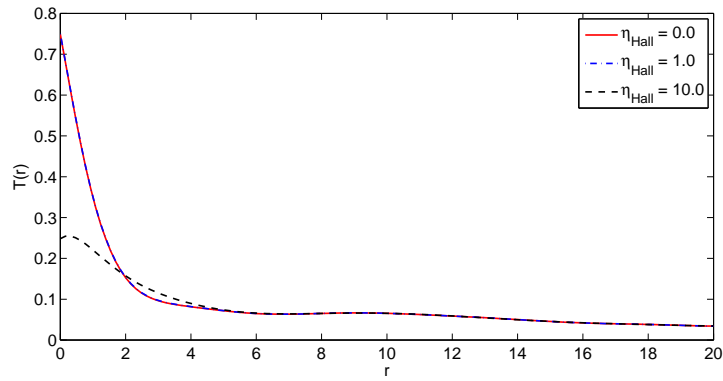


**Fig. 10** The temperature in the middle of the disk for  $\eta_{\text{Hall}} = 0.0$ ,  $\eta_{\text{Hall}} = 1.0$  and  $\eta_{\text{Hall}} = 10.0$  at time  $t = 250 \tau_{\text{K}0}$ .

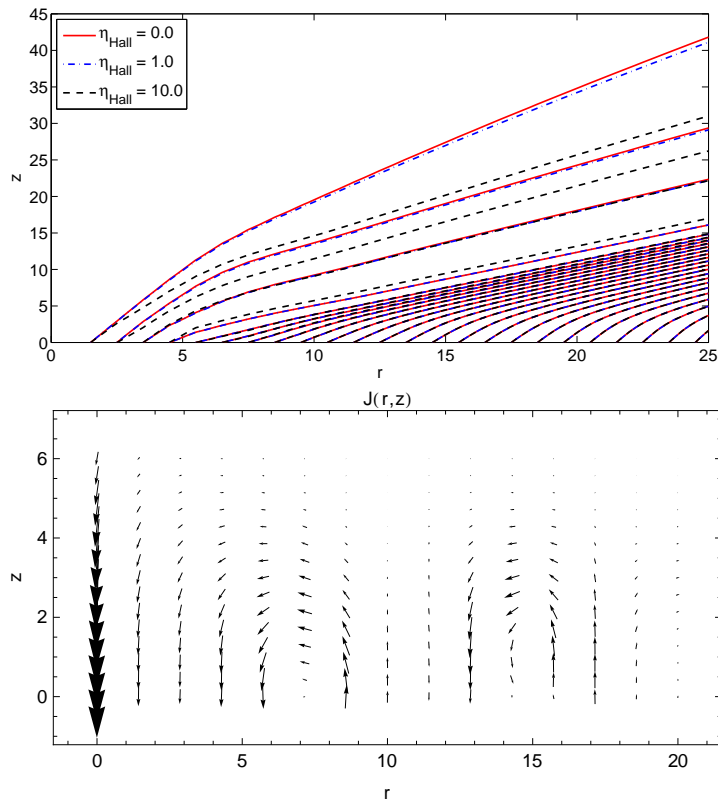


**Fig. 11** The vectorplot of the current density in the disk and the atmosphere (*lower panel*) and the magnetic field lines (*upper panel*) for  $\eta_{\text{Hall}} = 0.0$ ,  $\eta_{\text{Hall}} = 1.0$  and  $\eta_{\text{Hall}} = 10.0$  at time  $t = 250 \tau_{\text{K}0}$  (*solid, dot-dashed and dashed lines, respectively*).

The oscillating behavior of the induced toroidal magnetic field due to the Hall effect was previously reported by Shalybkov & Urpin (1997).

As is clear in Figure 5, the structure of the poloidal component of the magnetic field does not change significantly due to the Hall effect. The toroidal component of current density directly depends on variations in the poloidal component of the magnetic field with respect to radial distance. Hence, we expect that the toroidal current has larger values where the poloidal components of the B-field vary rapidly with respect to  $r$ .

In Figures 6 and 7 the  $r$ - and  $z$ - components of the field with respect to  $r$  are presented. They clearly show that these components are not significantly affected by the Hall parameter. As is clear from Figure 8, for different values of Hall coefficients, there is no change in the density of the accretion flow, but a high value of the Hall coefficient,  $\eta_{\text{Hall}} = 10.0$ , will significantly change the pressure of the disk, see Figure 9. Knowing the pressure and the density of the disk allows us to calculate the disk temperature at every point of a mesh grid, where the value of temperature as an output of the program is calculated.

Figure 10 shows the variation of temperature along the radius of the disk for the time when the Hall coefficient changes. For higher values of the Hall coefficient,  $\eta_{\text{Hall}} = 10.0$ , the temperature of the disk will decrease in the inner part of the disk as compared to the case where the Hall effect does not have any role, but for lower values of  $\eta_{\text{Hall}}$  there is no considerable change. Since Hall diffusion occurs when the magnetic field is strong, we expect to see its footprints in the inner part of the disk. In Figure 11 we have illustrated the vector plot and formation of current density inside the disk (lower panel) for  $\eta_{\text{Hall}} = 10.0$ . It is clear that the Hall coefficient has a greater effect inside the disk as compared to the outside and the surrounding atmosphere. Magnetic field lines, as shown in Figure 11 (upper panel) after time passes  $250 \tau$  for different coefficients, are illustrated. When Hall diffusion becomes more important by adding  $\eta_{\text{Hall}}$ , the magnetic field lines are curved toward the disk plane. For the magnetic field lines, which are at a lower angle with respect to the disk plane, changes due to Hall diffusion are not remarkable. This means that Hall diffusion mainly affects the outer magnetic field lines.

#### 4 CONCLUSIONS

In the accreting gas which is partially ionized, the magnetic field will freeze in an electron fluid due to resistivity. In this case non-ideal MHD should be taken into account. The difference in the mean electron velocity and the center-of-mass fluid velocity gives rise to a Hall effect in the accreting gas. It has been shown that in protoplanetary disks around young stars, the Hall diffusion can be important, and therefore must be taken into account in realistic models of such systems. In previous investigations, researchers usually ignored the Hall diffusion in the simulation of the protostellar disk because of its difficulty.

In this paper, we perform a 2.5D numerical simulation of a resistive accretion disk treated by a weak magnetized field by adding the Hall effect using the PLUTO code. In the formation and evolution of the protostellar disk, its size and rotational behavior, and the components of current density, magnetic diffusion, and in particular Hall diffusion, are clearly important. This simulation has been used to show that Hall diffusion can effectively change the dynamics of accretion flow in a protostellar disk.

In this simulation we take into account both the Hall diffusion and magnetic resistivity in an induction equation. We have shown that this relatively simple model can be used to explain the importance of Hall diffusion on the structure of a magnetized protostellar disk. The structure of the poloidal component of a magnetic field does not significantly change due the Hall effect.

We have shown that by adding  $\eta_{\text{Hall}}$ , the toroidal component of current density will shift to the inner part of the disk, but, when adding the Hall diffusion, a transverse current will penetrate with its amplitude increasing with an increasing Hall coefficient. The results show that the induced current

will be dampened far from the inner boundary of the disk, since the role of the magnetic field is dominant in the inner part of the disk.

It would be interesting to study the influence of Hall transverse resistance on outflow and wind in a future investigation to find out how this would change the solutions.

**Acknowledgements** We would like to thank the anonymous referee for her/his constructive suggestions and comments which were helpful for the improvement of this paper. We are grateful to the School of Astronomy at IPM for their computer facilities and financial support which helped us to perform numerical simulations.

## References

- Arlt, R., & Rüdiger, G. 2001, *A&A*, 374, 1035  
Balbus, S. A., & Hawley, J. F. 1991, *ApJ*, 376, 214  
Balbus, S. A., & Terquem, C. 2001, *ApJ*, 552, 235  
Braiding, C. R., & Wardle, M. 2012a, *MNRAS*, 422, 261  
Braiding, C. R., & Wardle, M. 2012b, *MNRAS*, 427, 3188  
Brandenburg, A., Nordlund, A., Stein, R. F., & Torkelsson, U. 1995, *ApJ*, 446, 741  
Frank, J., King, A., & Raine, D. J. 2002, *Accretion Power in Astrophysics: Third Edition* (Cambridge: Cambridge Univ. Press)  
Hawley, J. F., Gammie, C. F., & Balbus, S. A. 1995, *ApJ*, 440, 742  
Kitchatinov, L. L., & Rudiger, G. 1997, *MNRAS*, 286, 757  
Kluźniak, W., & Kita, D. 2000, arXiv:astro-ph/0006266  
Königl, A., Salmeron, R., & Wardle, M. 2010, *MNRAS*, 401, 479  
Liverts, E., Mond, M., & Chernin, A. D. 2007, *ApJ*, 666, 1226  
Matsumoto, R., & Tajima, T. 1995, *ApJ*, 445, 767  
Mellon, R. R., & Li, Z.-Y. 2008, *ApJ*, 681, 1356  
Mignone, A., Bodo, G., Massaglia, S., et al. 2007, *ApJS*, 170, 228  
Murphy, G. C., Ferreira, J., & Zanni, C. 2010, *A&A*, 512, A82  
Price, D. J., & Bate, M. R. 2007, *MNRAS*, 377, 77  
Regev, O., & Gitelman, L. 2002, *A&A*, 396, 623  
Sano, T., & Stone, J. M. 2002a, *ApJ*, 570, 314  
Sano, T., & Stone, J. M. 2002b, *ApJ*, 577, 534  
Shadmehri, M. 2012, *Ap&SS*, 338, 151  
Shakura, N. I., & Sunyaev, R. A. 1973, *A&A*, 24, 337  
Shalybkov, D. A., & Urpin, V. A. 1997, *A&A*, 321, 685  
Torkelsson, U., Brandenburg, A., Nordlund, Å., & Stein, R. F. 1996, *Astrophysical Letters and Communications*, 34, 383  
Umurhan, O. M., Nemirovsky, A., Regev, O., & Shaviv, G. 2006, *A&A*, 446, 1  
Urpin, V. A. 1996, *MNRAS*, 280, 149  
Wardle, M. 1999, *MNRAS*, 307, 849  
Wardle, M. 2004, *Ap&SS*, 292, 317  
Zanni, C., & Ferreira, J. 2009, *A&A*, 508, 1117